Rocznik Ochrona Środowiska
Volume 28 Year 2026 ISSN 2720-7501 pp. 658-672
https://doi.org/10.54740/ros.2026.044 open access
Received: June 2026 Accepted: July 2026 Published: August 2026

Effect of Relative Draft and Mooring Configuration on Wave Transmission of Rectangular Floating Breakwater

Teeba M. Yehia, Abdul-Hassan K. Al-Shukur*
Department of Civil Engineering, College of Engineering, Babylon University, Hilla, Iraq
corresponding author's email: sth.tiba.ibrahim@student.uobabylon.edu.iq

Abstract: Background: Floating breakwaters (FBs) have gained increasing attention as cost-effective and environmentally friendly alternatives to conventional bottom-founded coastal protection structures. Their wave attenuation performance is critically influenced by geometric and hydrodynamic parameters, among which draft and structural width are of primary importance. Despite extensive research, the combined influence of non-dimensional relative draft parameters and mooring configuration on wave transmission has not been thoroughly investigated in an integrated experimental framework. Materials and Methods: This study presents a systematic experimental investigation into the effects of draft (D), relative draft to model width (D/B), relative draft to wavelength (D/L), and relative draft to incident wave height (D/Hi) on the wave transmission coefficient (Kt) of rectangular pontoon-type floating breakwaters. Three models of different widths were tested under ten regular wave conditions, with five draft values and two chain mooring configurations (parallel and cross), yielding a total of 300 experimental tests conducted in a laboratory wave flume. Results and Discussion: The main results were that increasing draft consistently reduced Kt across all tested conditions, with reductions of up to 80% at the maximum draft. Among the three relative draft parameters, D/L proved to be the most reliable predictor of Kt, with an average Pearson correlation coefficient of $|r| = 0.646$ and $R^2 = 0.430$. The widest model achieved the best overall wave attenuation performance. For D/Hi, a direct (positive) relationship with Kt was observed, where lower D/Hi values produced greater wave-structure interaction and more effective attenuation. The cross-mooring arrangement generally yielded lower Kt values than the parallel arrangement, with an overall average difference of 7.15%. Conclusion: D/L is recommended as the primary non-dimensional design parameter for rectangular floating breakwaters, while D/Hi serves as a useful complementary indicator. The findings provide practical guidance for the design of rectangular floating breakwaters in coastal protection applications.

Keywords: floating breakwaters, wave transmission coefficient, relative draft, mooring configuration; coastal protection

1. Introduction

Breakwaters, sometimes referred to as wave attenuators, are frequently considered as coastal structures that limit the action of waves in inshore seas, hence reducing coastal erosion and offering safe harborage (Dai et al., 2018). In general, they could be categorized as bottom-founded breakwaters, floating breakwaters, and composite breakwaters. Traditional bottom-founded breakwaters are trapezoidal or rectangular in shape to withstand the bottom overturning moment. It is obvious that the wave energy distribution throughout the water depth is incompatible with the section's variation (and, consequently, the building materials).

The floating breakwater (FB) offers several significant advantages over traditional bottom-founded structures, as it provides a reasonable alternative because its main body is close to the free surface (Wang et al., 2025). The main advantages of floating breakwaters include their cost-effectiveness, environmental friendliness, ease of installation, and suitability for areas with poor foundation conditions, as they are less expensive than bottom-founded structures, promote water exchange to support marine ecosystems, and can be installed more quickly and simply. Still, the main problem with them is their low efficiency against long waves. (Abasi et al., 2023; Ji et al., 2019). These features make floating breakwaters a practical, economical, and environmentally conscious option for coastal protection, especially in challenging conditions.

Floating breakwaters' attenuating ability is a key area for research and development, especially to attenuate short and immediate wave periods; the remaining challenge is resisting long-period waves. Many studies have found that the draft (D, which is the submergence percentage of the floating body or the submerged height) increases the floating breakwater efficiency to become more effective in wave attenuation in the form of a lower transmission coefficient (Kt) value for most wave conditions. The role of draft in governing the wave transmission performance of floating breakwaters has been the subject of several experimental and numerical investigations. Duan et al. (2017) examined an F-type floating breakwater and demonstrated that a higher draft depth results in a noticeable decrease in Kt, which is explained by the submerged body's increased obstruction of wave orbital motion. Chen et al. (2020) discovered that increased submergence increases wave reflection at the incident face and decreases the fraction of energy delivered to the lee side for a pile-restrained WEC-type floating breakwater. Nasri et al. (2021) developed this to trapezoidal pontoon breakwaters equipped with porous plates, finding that one of the most important geometric factors influencing transmission performance is draft, which is more noticeable at shorter wave periods. Rajabi and Ghassemi (2021) compared five different cross-sectional shapes and noted that, across all configurations tested, increasing draft consistently improved wave attenuation, with the rectangular section showing a particularly clear and predictable response. Saie et al. (2023) confirmed the inverse relationship between draft and Kt for a novel floating breakwater configuration tested under regular wave conditions in a laboratory flume.

Beyond draft, the relative width of the floating breakwater with respect to the incident wavelength (B/L) has been widely recognized as a key non-dimensional parameter governing wave transmission. Larger B/L ratios generally result in lower transmission coefficients, as a wider structure intercepts more wave energy (Nikpour et al., 2019). Furthermore, Cheng et al. (2025) and Y. Wang et al. (2025) confirmed theoretically that the wave period and breakwater draft, along with relative width (B/L), are the main factors influencing Kt of the rectangular floating breakwaters. However, the combined effect of mooring configuration and relative draft D/B, D/L, and D/Hi (where Hi is the incident wave height, B is the width of a floating breakwater, and L is the wavelength) on wave transmission has not been thoroughly investigated in an integrated experimental framework.

The mooring system of a floating breakwater plays a crucial role not only in station-keeping but also in influencing the dynamic response and wave attenuation performance of the structure (Sannasiraj et al., 1998). Different mooring configurations alter the restoring forces and motion response of the breakwater, which in turn affects the wave transmission characteristics. Lee and Ong (2025) and Xu et al. (2024) investigated the numerical behavior of different mooring formations. Still, despite these findings, a direct experimental comparison between parallel and cross mooring chain arrangements under systematically varied draft and width conditions remains limited in the literature. Despite the extensive research conducted on floating breakwaters, a clear gap exists in the literature regarding the combined effect of non-dimensional draft ratios (D/B and D/L) and mooring configuration on the wave transmission coefficient of rectangular floating breakwaters. Most previous studies investigated these parameters independently, without examining their interaction under controlled laboratory conditions. Furthermore, the non-dimensional parameter D/Hi, which directly relates the structural draft to the incident wave height, has received limited attention as a predictor of Kt in rectangular pontoon floating breakwaters. Additionally, comparative experimental studies between parallel and cross mooring chain arrangements under systematically varied draft and width conditions remain limited. This study addresses these gaps through a systematic experimental investigation supported by statistical analysis.

The present study offers three main contributions to the existing literature on floating breakwater performance. First, it provides a systematic experimental comparison of the non-dimensional relative draft parameters D/B and D/L as predictors of the wave transmission coefficient, supported by statistical analysis using the coefficient of determination (R^2). Second, it presents a direct experimental comparison of parallel and cross chain mooring configurations across a comprehensive range of structural widths, draft values, and wave conditions. Third, it introduces D/Hi as an additional non-dimensional parameter that directly links the structural submergence depth to the energy-carrying wave height, providing a complementary perspective on wave-structure interaction. An experimental method was used to examine the effect of draft and relative draft on the wave transmission coefficient for three rectangular floating breakwater models with varying widths. A thorough dataset for assessing the hydrodynamic efficiency of rectangular floating breakwaters was obtained by using two mooring configurations (parallel and cross chain arrangements) to examine their impact on draft and relative draft performance under ten various regular wave conditions.

2. Experimental Work

This part shows the experimental equipment and model used in the experiments. It also states the steps taken to carry out the experimental work.

2.1. Wave Flume and Experimental Facility

The experiments were conducted in a wave flume measuring 10 m in length, 1m in width, and 1 m in depth, as illustrated in Fig. 1. The flume walls are constructed of 10 mm thick transparent glass panels, which allow visual observation of wave interactions with the model during testing. Steel structural frames reinforce the glass panels to ensure structural rigidity throughout the experimental runs.

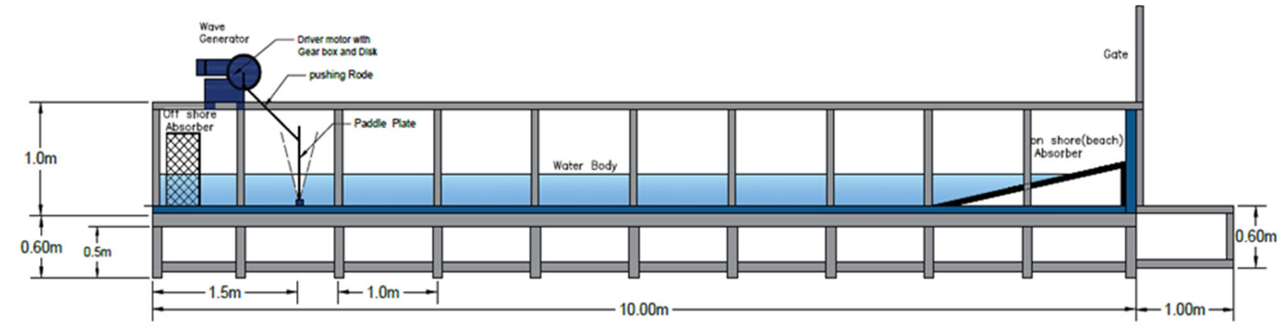

Fig. 1. Sketch of wave flume

A flap-type wavemaker is installed at one end of the flume and can generate regular waves over a wide range of wave periods and heights. The wavemaker is driven by a 3HP three-phase induction motor operating at 50Hz. The motor is connected to the power supply through a control unit equipped with an inverter, which allows precise adjustment of the motor speed and, consequently, the generated wave characteristics. The oscillatory motion of the paddle creates waves mechanically by displacing water at the free surface to create the required wave patterns. A wide variety of short to intermediate wave conditions pertinent to floating breakwater applications were covered by the produced wave durations, which varied from 0.65 to 2.2 s.

Two passive wave absorption systems were used to reduce wave reflection and guarantee measurement accuracy. To absorb any reflected waves from the offshore boundary, an offshore absorber, a vertical box filled with gravel, was positioned at the base of the flume behind the wavemaker. At the other end of the flume, close to the terminal border, was an onshore absorber. To efficiently disperse the energy of transmitted waves and minimize re-reflection, this absorber is made up of a perforated plate inclined at a 1:4 slope, chosen in accordance with the flume dimensions. Each experimental run has a maximum duration of 60 s to ensure that, during the measurement period, incident and transmitted wave signals were unaffected by wave reflections from the two absorbers (Nikpour et al., 2019).

The floating breakwater model was positioned at the midpoint, between the wavemaker paddle and the onshore wave absorber. At equal distances, four ultrasonic wave gauges were installed along the flume, two on each side, before and after the physical FB model, to record water surface variation in water surface elevation at a sampling frequency of 30Hz. The gauges were placed to capture both the incident and transmitted wave heights, enabling data analysis and calculation of Kt for each experimental condition. A comprehensive overview of the experimental setup is presented in Fig. 2.

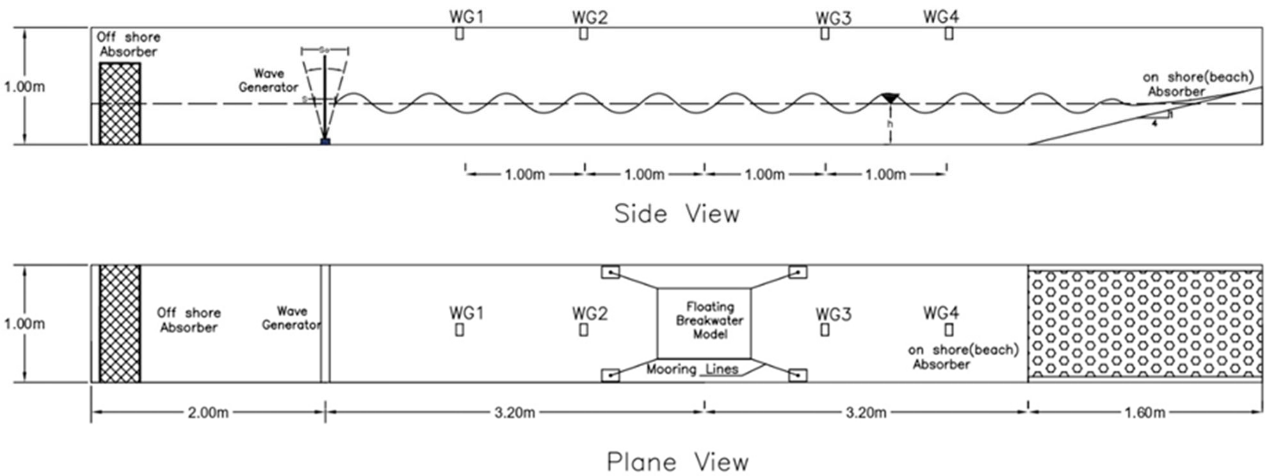

Fig. 2. Sketch of wave flume and experimental setup

2.2 Tested Models

Three rectangular pontoon-type floating breakwater models were investigated in the present experimental study. All models share the same length (l = 0.8 m) and total height (H = 0.30 m), while the width (B), facing the incident wave, was systematically varied across the three models to examine its effect on wave transmission performance. The geometric dimensions of all tested models are summarized in Table 1 and illustrated in Fig. 3.

Table 1. Dimensions of the tested rectangular pontoon floating breakwater models

Model	B (m)	l (m)	H (m)	D (m)
R1	0.6	0.8	0.30	0.04–0.20
R2	0.8	0.8	0.30	0.04–0.20
R3	0.9	0.8	0.30	0.04–0.20

All three models were hollow, manufactured using transparent glass sheets that were 4mm thick to offer sufficient structural rigidity and allow for visual observation of wave-structure interaction during testing. It was then framed into a lightweight steel structure to make it easier to connect mooring chains during setup.

The experimental work was established to systematically investigate the effects of draft (D) and relative draft ratios (D/B, D/L and D/Hi) on the wave transmission coefficient (Kt). Water was added into the model from a known volume to meet the selected draft for each set of experiments. For each model, draft varied from 0.04 m to 0.20 m in five increments: 0.04, 0.08, 0.12, 0.16, and 0.20 m, representing a percentage of submergence depths that ranges from approximately 13 percent to 67 percent of the model's overall height. This range was chosen to capture the transition from shallow to deep submergence relevant to practical floating breakwater applications.

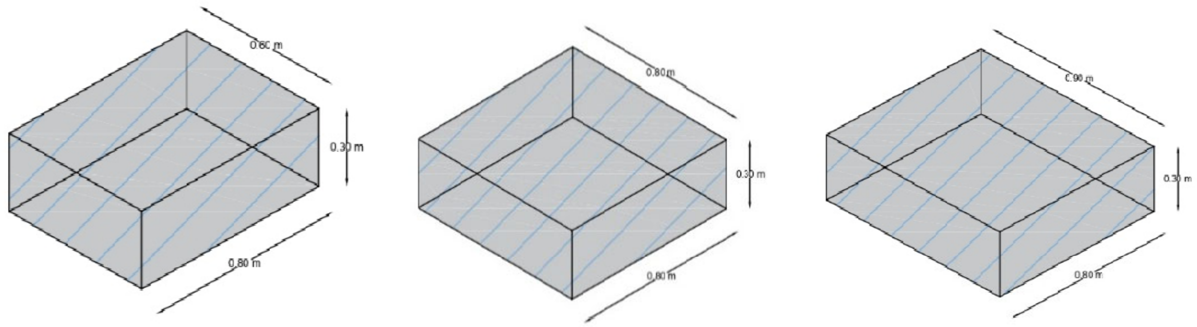

R1 R2 R3

Fig. 3. Sketch of the three models studied

2.3. Wave Conditions

Ten distinct regular wave circumstances, comprising a wide variety of wave heights and periods crucial to the assessment of FB performance, were used in this experimental work. In all investigated models, the incidence wave heights (Hi) vary between 0.024 m and 0.24 m, the water depth ($d \approx 0.35$ m) is fixed.

It is noticeable that the actual wave properties observed during each experimental run varied according to the wave-structure interaction for all models under examination. Because the FB model in the flume alters the local wave field, each model configuration has somewhat different incident wave heights and lengths at the same paddle frequency setting. To guarantee precise and representative values of (Hi) and wave period (T) for each of the experimental tests carried out on the three rectangular models, the wave parameters were measured individually for each experimental run using the installed ultrasonic wave gauges.

The systematic variation of wave conditions, along with the three model widths and five draft values tested under two mooring configurations, resulted in a comprehensive experimental dataset of 300 individual tests, providing a strong basis for investigating the impact of draft and relative draft on wave transmission.

2.4. Mooring System

Two mooring configurations were investigated in this study to examine their influence on the wave transmission performance of rectangular FB models. In both configurations, the model was restrained using four steel chains, each with a total length of 1.2 m, with two chains attached to the incident (wave-facing) side of the model, and two chains attached to the transmitted (lee) side. The upper ends of the chains were connected to the light-steel frame of the FB model, while the lower ends were anchored to fixed steel anchor plates embedded in the flume bed. The effective length of the deployed chains varied depending on the width of the tested model. During still-water testing conditions, the mooring chains were not tensioned, resulting in the floating breakwater model being free to move within the limits of the chain length. In this way, the mooring chains will be in a slack position until they are displaced by the wave motion, creating a force resisting forward movement while allowing heave and pitch responses.

In the parallel mooring, the four chains are oriented parallel to one another. The two chains on the incident side connect directly to two anchor points on the same side of the flume bed, and similarly, the two chains on the transmitted side connect to their respective anchor points on the lee side. This configuration provides symmetric and direct lateral restraint on both sides of the model, as illustrated in Fig. 4a.

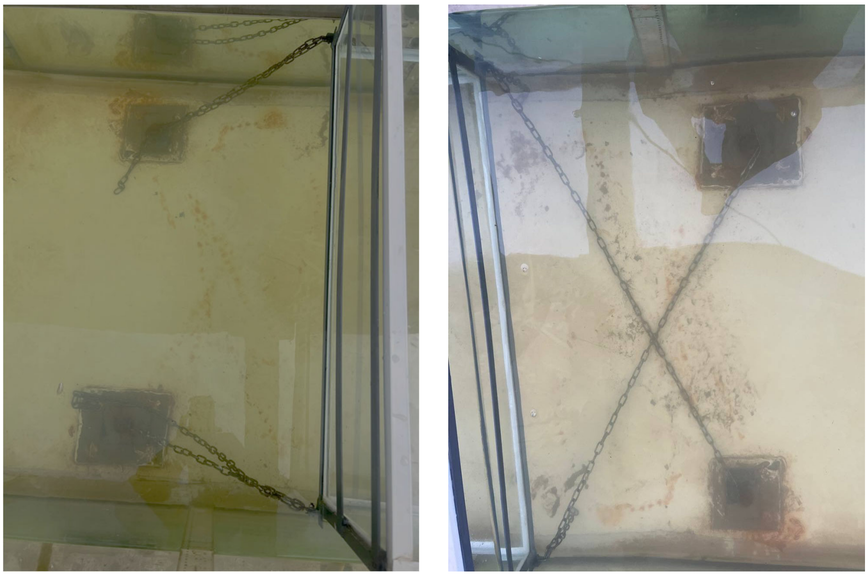

(a) Parallel mooring system (b) Cross- mooring system

Fig. 4. Mooring lines configuration. (a) Parallel mooring system. (b) Cross-mooring system

In the cross-mooring arrangement, the chains are oriented diagonally, forming an X-pattern when viewed from above. In this configuration, each chain connects one side of the model frame to an anchor point on the opposite side of the flume bed. The two configurations were tested under identical conditions to enable a direct empirical comparison of their effects on wave transmission performance, without the use of motion-response instrumentation in the present study. The cross-mooring arrangement is illustrated in Fig. 4b.

Both mooring configurations were tested under identical wave and model conditions, to enable a direct and systematic comparison of their effects on Kt. All experimental tests were conducted for both arrangements across the full range of model widths, draft values, and wave conditions investigated in this study.

2.5. Data Analysis

The zero up-crossing approach was used to analyze the recorded experimental waves for each of the 300 experiments, extracted from wave gauges. Following analysis, incident wave and transmitted wave heights, Hi and Ht, respectively, as well as wave periods, consequently wavelengths and Kt were then calculated using equations (1) and (2), respectively.

$$L = \frac{g\,T^2}{2\pi} \tag{1}$$

$$Kt = \frac{H_t}{H_i} \tag{2}$$

where Kt denotes the transmission coefficient, which is dimensionless; L, is the wavelength measured in (m), and g is the gravitational acceleration (m/s^2). The wave transmission coefficient Kt is an important parameter for the wave attenuation performance of the FB (Shen et al., 2022). The wave transmission coefficient Kt is the ratio of the transmitted wave height behind the FB to the incident wave height in front of the FB.

3. Results and Discussion

3.1. Effect of Draft

The influence of the FB draft on the wave transmission coefficient for the same wave maker frequency for a rectangular FB is shown in Figs. (5) to (7) indicate that as the structural draft increases, the transmission coefficient progressively decreases for all three tested models and both mooring configurations. Lower Kt values were generally observed at larger draft depths, particularly at D = 16 cm and D = 20 cm, compared with smaller draft values such as D = 4 cm and D = 8 cm, confirming it is a key parameter for lowering wave transmission of rectangular FBs.

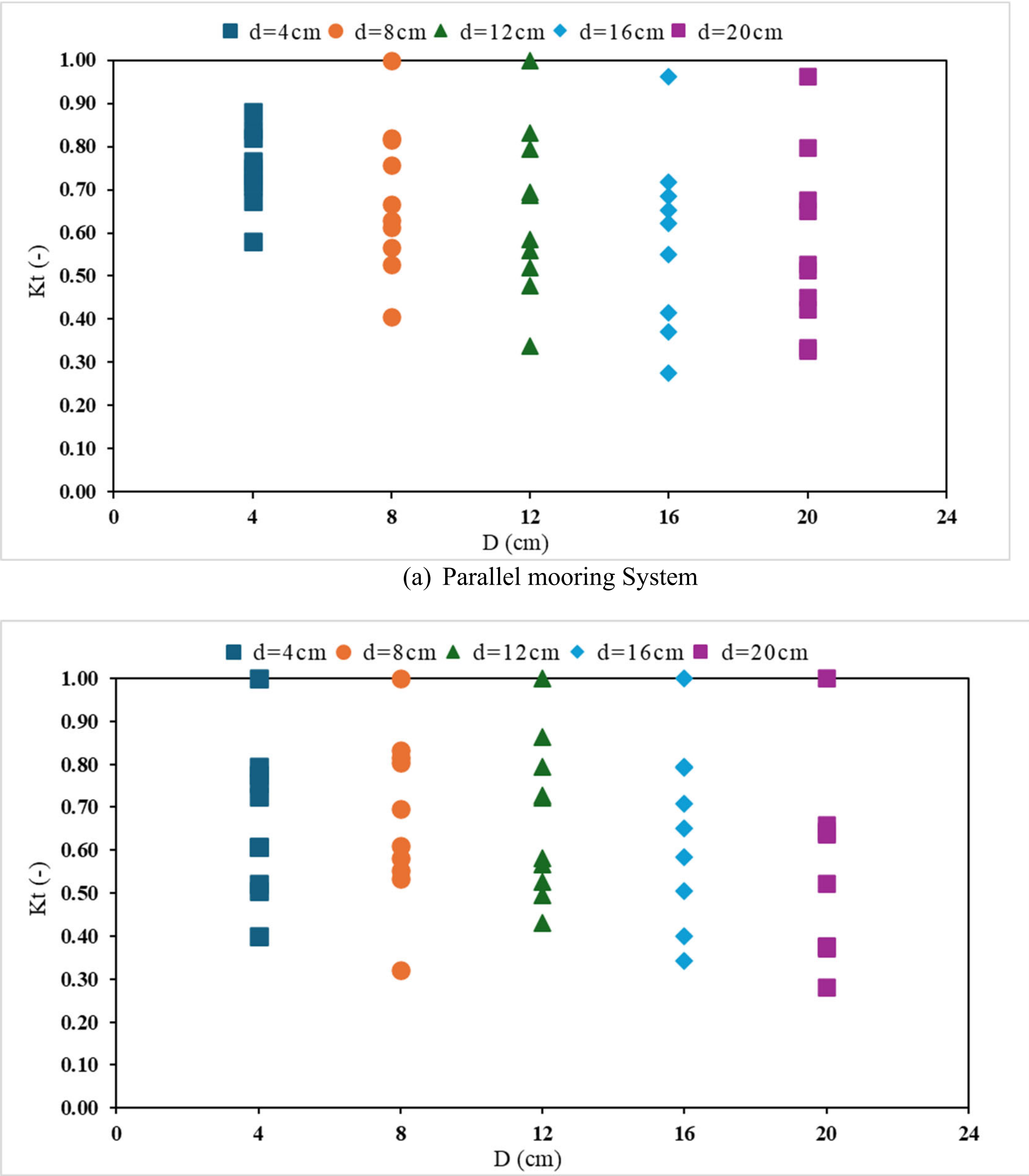

(a) Parallel mooring System

(b) Cross mooring System

Fig. 5. Transmission coefficient versus draft (D) for model R1. (a) Parallel mooring system. (b) Cross- mooring system

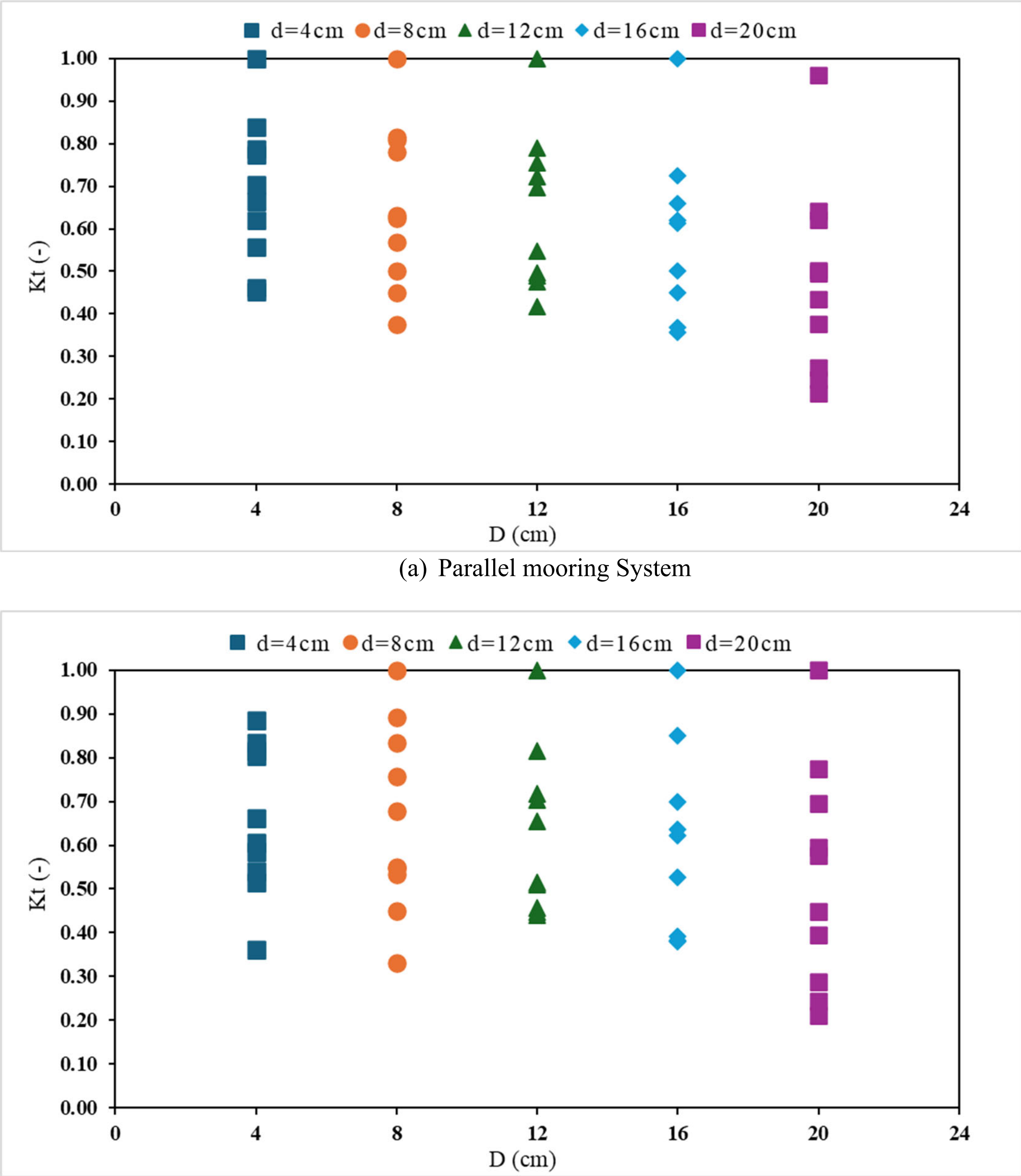

(a) Parallel mooring System

(b) Cross mooring System

Fig. 6. Transmission coefficient versus draft (D) for model R2. (a) Parallel mooring system. (b) Cross- mooring system

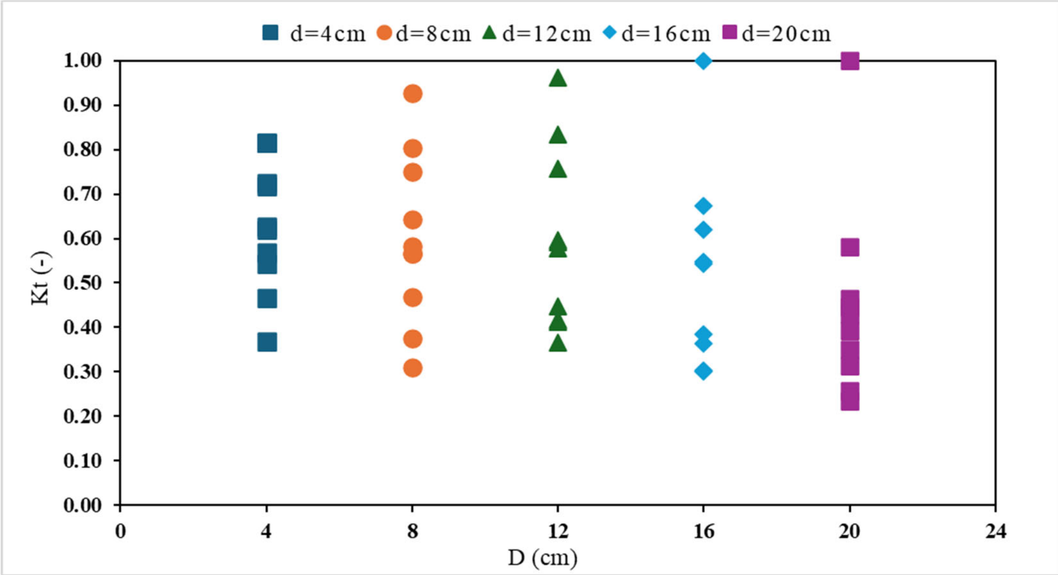

(a) Parallel mooring System

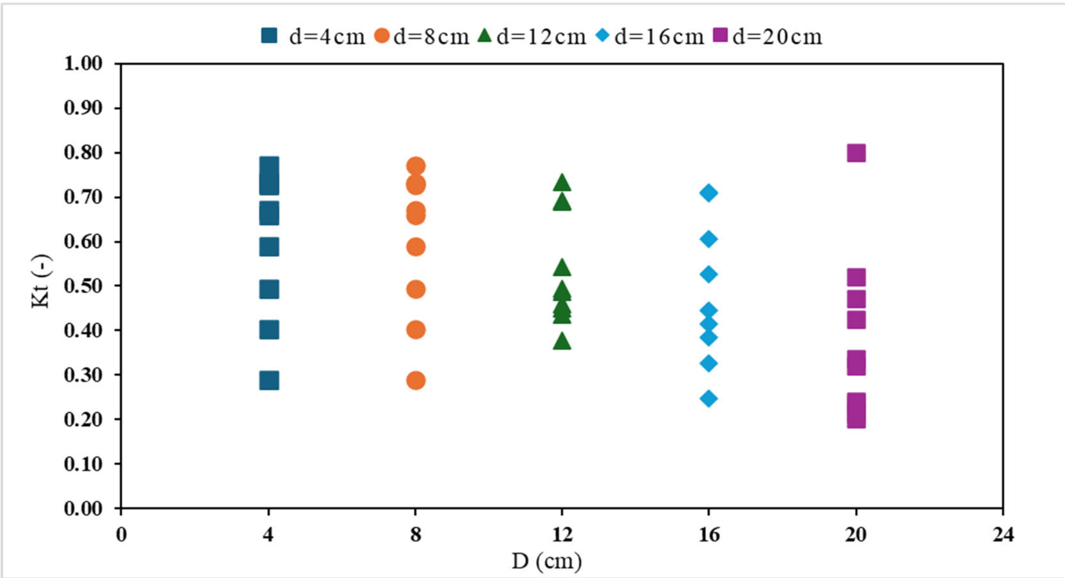

(b) Cross mooring System

Fig. 7. Transmission coefficient versus draft (D) for model R3. (a) Parallel mooring system. (b) Cross- mooring system

This decrease is caused by the breakwater's increased submerged section, which improves its interaction with the active incident waves zone and, as a result, its wave attenuation performance. This increase in the structure's draft places more of its body in water and can effectively stop wave energy from passing through the bottom of the structure. Increasing the structural draft also increases the mass and inertia of the system, leading to greater wave energy dissipation. Nikpour et al. (2019) identified the same mechanism and confirmed that draft is among the most influential parameters governing Kt in trapezoidal floating breakwaters tested under regular wave conditions. Similarly, Nasri et al. (2021) identified the same mechanism by conducting an experimental investigation of trapezoidal floating breakwaters with porous plates, observing that turbulence and wave reflection are increased with deeper draft, dissipating more incident wave energy.

For smaller draft values (D = 4 cm and D = 8 cm), the floating breakwater interacts with a relatively limited portion of the water column, allowing a larger amount of wave energy to pass beneath the structure. This explains the relatively high Kt values obtained with low draft values, particularly for relatively longer wave periods, where velocities extend deeper into the water column. On the other hand, the structure intercepts a significantly greater portion of the wave at the maximum draft tested (D = 20 cm), which represents approximately 67 percent of the model height. This is in line with the results of Shen et al. (2022), who found similar decreases in Kt with increasing relative draft depth in twin-pontoon floating breakwater with porous vertical plates, and identified draft as a primary governing parameter for floating breakwater performance.

3.2. Effect of (D/B) on Kt

The wave transmission coefficient (Kt) is presented as a function of the relative draft (D/B), for the three rectangular floating breakwater models (R1, R2, and R3), under both parallel and cross mooring configurations, in Figs. (8a) and (8b), respectively. The relative draft D/B, the ratio of submerged depth to model width, is a crucial non-dimensional parameter that combines the effects of structural width and draft on wave attenuation performance. By expressing the results in terms of D/B, the data from the three models can be plotted on a unified axis, enabling comparison of their hydrodynamic performance.

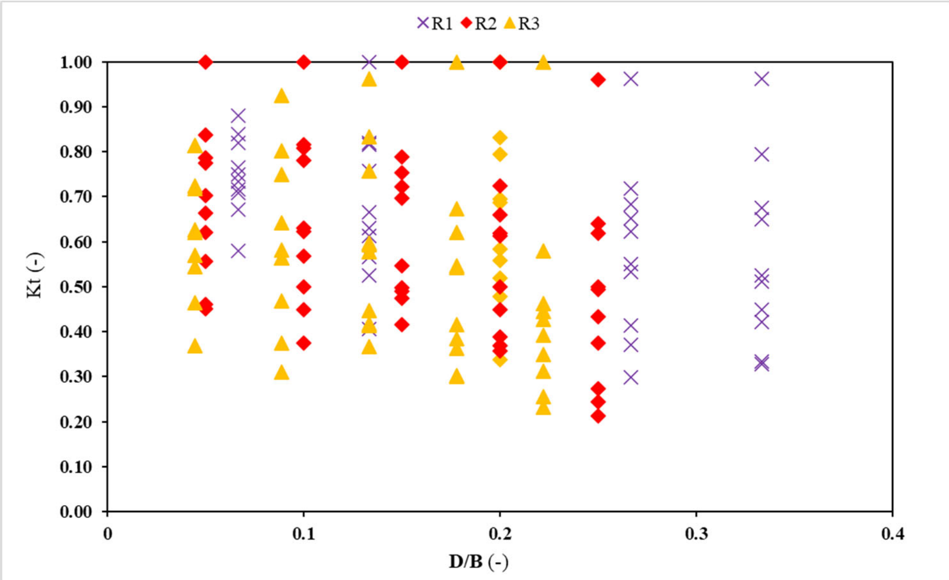

(a) Parallel mooring System

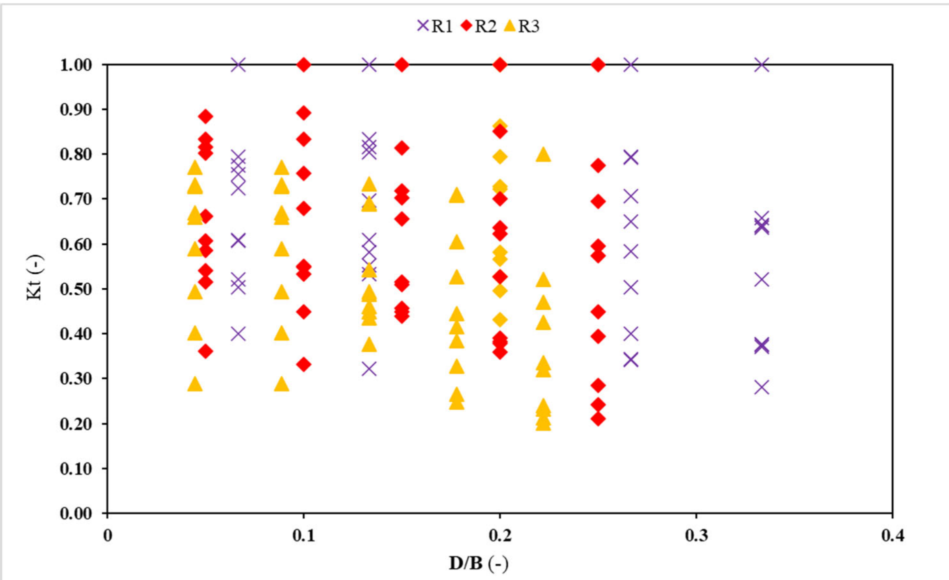

(b) Cross mooring System

Fig. 8. Transmission coefficient versus (D/B) for all the tested models. (a) Parallel mooring System. (b) Cross mooring System

The results show a clear inverse relationship between D/B and Kt for all three models and both mooring configurations. As D/B increases, Kt gradually drops, proving that better wave attenuation results from increased relative draft. In this study, D/B values covered a broad range of relative draft circumstances, from roughly 0.044 (D = 4 cm, R3) to 0.333 (D = 20 cm, R1).

Under parallel mooring (Fig. 8a), the transmission coefficient at the lowest D/B value ranged from approximately 0.37 to 0.81 across the three models, reflecting high wave transmission at shallow draft, for almost all wave conditions. At highest D/B values, Kt reduced to as low as 0.33 to 0.96 but not for all wave conditions, demonstrating a significant improvement in wave attenuation with increasing relative draft, especially for relatively short to medium wave periods.

For cross-mooring (Fig. 8b), a similar trend was observed, with Kt values ranging from 0.29 to 0.77 at low D/B, for almost all wave conditions, and decreasing to 0.28 to 1 at high D/B values, still not for all wave conditions. At equivalent D/B ratios, the cross-mooring arrangement consistently produced lower Kt values, indicating that the diagonal chain configuration adds more longitudinal restrictions, restricting wave energy transmission by minimizing surge and heaving motions. As no motion-response data were recorded, this trend is interpreted empirically. It is broadly consistent with the numerical results of Lee and Ong (2025), who demonstrate that the mooring configuration significantly influences the motion response of floating coastal structures under combined loading.

When comparing the three models at equivalent D/B values, it is evident that R1 exhibits higher Kt values than R2 and R3 across the full range of D/B tested. This suggests that models (R2 and R3) offer more wave attenuation for the same relative draft. Regardless of the submergence ratio, a wider structure absorbs more wave energy, which explains this pattern. As evidenced by the consistently low Kt values of R3 at high D/B, the combined impact of greater width and higher relative draft (D/B) results in the most effective wave attenuation. Ren et al. (2021) also observed that the structural width of pontoon breakwaters has a significant effect on wave attenuation that goes beyond what draft-based parameters can predict.

At low D/B ratios, there is a noticeable scatter in Kt values, especially for R1, whose narrow width allows it to reach the largest D/B range (up to 0.333). This scatter demonstrates the strong dependence of wave transmission on incident wave parameters at low draft. For both models, the scatter gradually decreases as D/B rises, suggesting that higher values offer more reliable wave attenuation performance over a larger range of wave circumstances. These findings are useful for FB design because they suggest that targeting higher D/B ratios can lead to more reliable and predictable wave protection.

3.3. Effect of (D/L) on Kt

The relationship between wave transmission coefficient (Kt) and relative draft (D/L) is presented in Figs. (9a) and (9b) for the parallel and cross mooring, respectively. In contrast to D/B, which relates the draft to the structural width, D/L captures the interaction between the FB draft and wavelength, making it a particularly meaningful parameter for characterizing wave-structure interaction. Greater D/L values show that the structure occupies up a greater portion of the wavelength in the vertical direction, which is associated with greater wave energy interception and dissipation.

Results show that D/L and Kt have a significant and consistent inverse relationship in all three models and both mooring configurations. As D/L increases, Kt decreases progressively and is notably less scattered, compared to D/B results. This reduced scatter suggests that D/L is a stronger governing parameter than D/B for predicting wave transmission through rectangular FB, as it simultaneously accounts for both the submergence depth and the wave characteristics.

Under the parallel mooring (Fig. 9a), Kt values ranged from approximately 0.45 to 1 at the lowest D/L values (average D/L ≈ 0.02) and decreased to 0.23 to 1 at the highest D/L values (average D/L ≈ 0.12). The three models' data points exhibit a comparatively consistent decreasing trend, confirming the effectiveness of D/L as a unifying non-dimensional parameter.

The cross-mooring (Fig. 9b) exhibited a very similar trend to the parallel mooring, with Kt values following closely comparable distributions across the full range of D/L. The close similarity between the two Figs. indicates that the influence of mooring configuration on Kt when expressed as a function of D/L is relatively minor. This suggests that, from an empirical standpoint, the wave transmission behavior characterized by D/L is relatively insensitive to the mooring arrangement tested in this study. Minor differences between the two configurations, however, are still discernible at intermediate D/L values, where the cross mooring tends to yield slightly lower Kt. Consequently, designing a draft that is a significant fraction of the target wavelength enhances wave attenuation and energy capture, whereas a draft much smaller than the wavelength provides little hydrodynamic benefit. Cheng et al. (2022) similarly found that D/L is a more reliable predictor of wave attenuation in floating breakwaters of the pontoon type. They noted that, to achieve efficient wave protection, structural draft should preferably represent a considerable fraction of the incident wavelength.

With equivalent D/L ratios, R3 consistently showed the lowest Kt values among the three models, followed by R2 and R1. Because R3 has the largest width (B = 0.9 m), which contributes to additional wave energy dissipation beyond what is recorded by D/L alone, this ordering shows the combined influence of both draft and model width. When plotted against D/L, the three models do not collapse onto a single curve, indicating that B is still a significant independent factor that should be considered in addition to D/L when designing rectangular floating breakwaters. Wang et al. (2025) arrived at a similar conclusion in their theoretical study of rectangular floating breakwaters, showing that the transmission coefficient is influenced independently by both the draft and the relative width B/L.

When comparing the results of D/L in Fig. (9) with those of D/B in Fig. (8), it is evident that D/L provides a more distinct and consistent trend with less data scattering. These findings demonstrate that, under a range of structure widths and wave conditions, D/L is a more accurate non-dimensional parameter for characterizing how well rectangular FB attenuates waves.

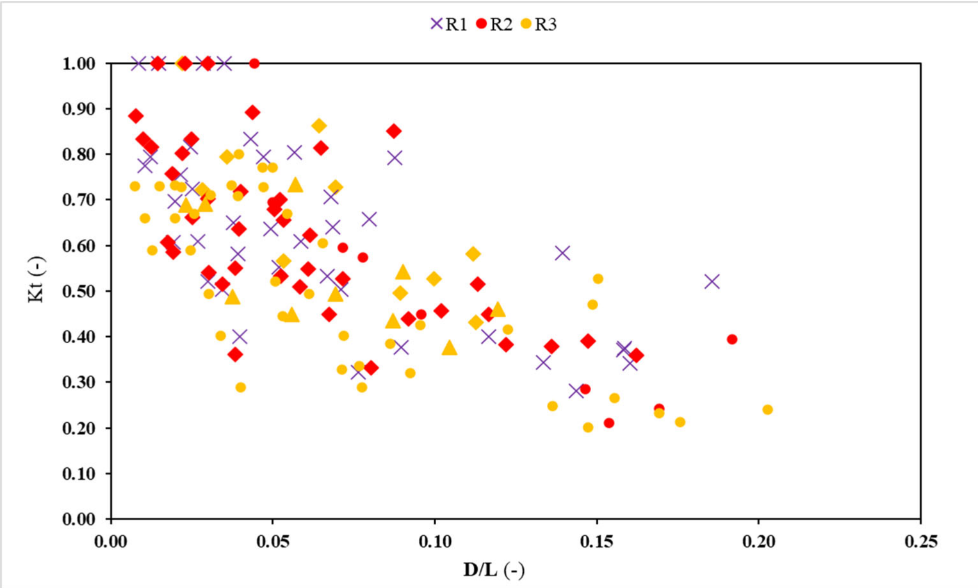

(a) Parallel mooring System

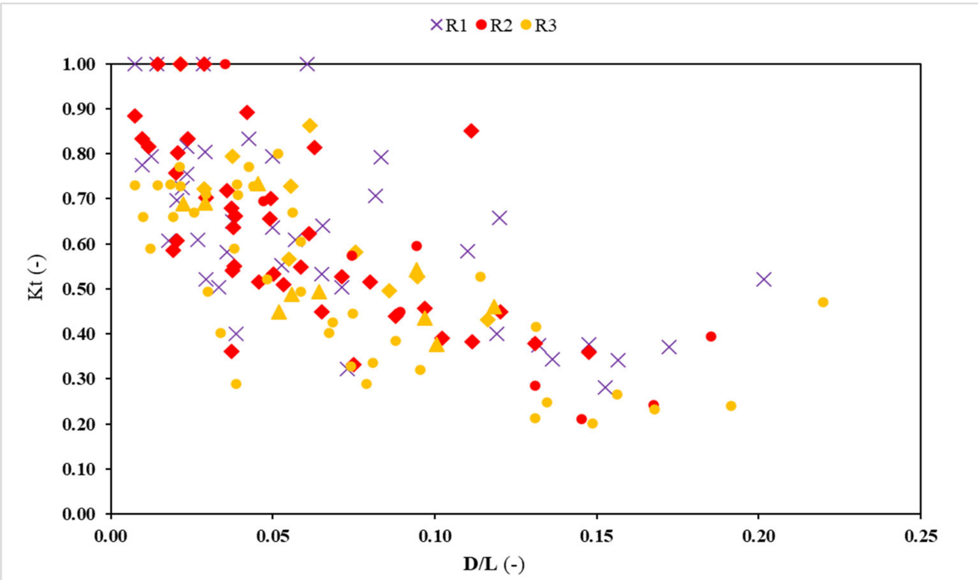

(b) Cross mooring System

Fig. 9. Transmission coefficient versus (D/L) for all the tested models. (a) Parallel mooring System. (b) Cross mooring System

3.4. Effect of (D/Hi) on Kt

This section introduces another non-dimensional parameter (D/Hi) to characterize the wave transmission capability of the rectangular floating breakwaters. Unlike D/B and D/L, which relate the draft to the structural scale and wavelength scale, respectively, the D/Hi ratio directly relates the draft to the incident wave height and can be used to quantify the ratio of the submerged depth of the breakwater to the height of the energy-carrying wave. The greater the D/Hi number, the larger the draft is in relation to the incident wave height, which means that the breakwater is in a larger proportion of the active wave zone and can, therefore, intercept more energy from the waves. Conversely, if the D/Hi number is less than one, then the wave height will dominate over the draft and, therefore, a larger amount of the incident energy will be transmitted below the breakwater.

Figs. (10a) and (10b) show the relationship between Kt and D/Hi for the three models under parallel and cross mooring configurations, respectively. The results demonstrate a direct (positive) relationship between D/Hi and Kt across all tested models and both mooring configurations; as D/Hi increases, Kt increases. This is physically consistent with the wave energy distribution theory: when the draft is large relative to the incident wave height, the incident wave is comparatively small and passes more freely past the structure with minimal attenuation. Conversely, when D/Hi is small (i.e., the incident wave height is large relative to the draft), the wave energy is concentrated in the zone occupied by the breakwater, leading to greater interaction and lower Kt.

In the parallel mooring configuration (Fig. 10a), the D/Hi values ranged from approximately 0.25 to 8, depending on the testing conditions. For the lower range of D/Hi where the incident wave height is much greater than the draft, Kt ranges from approximately 0.20 to 0.80, indicating greater interaction between the waves and the structure, resulting in more effective wave attenuation. The Kt values increased as D/Hi increased, reaching values as high as 1.0. Therefore, when the draft is much smaller than the wave height, the wave can pass freely by the structure with little or no attenuation.

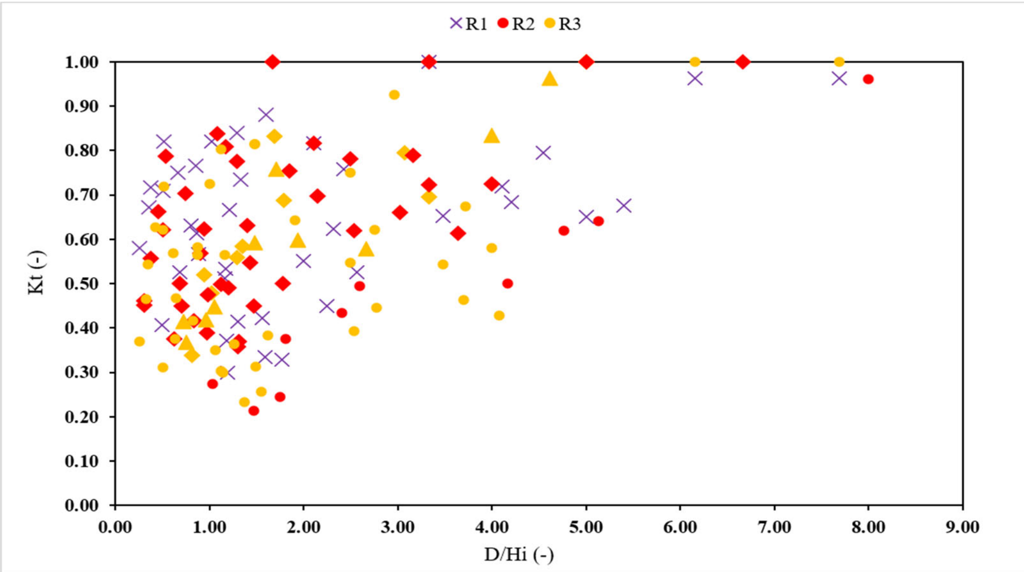

(a) Parallel mooring System

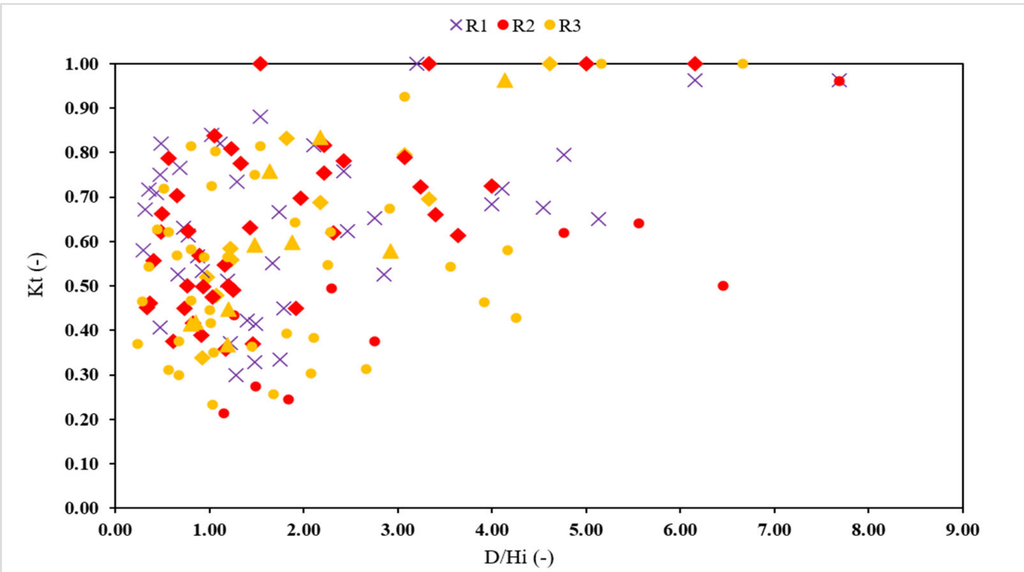

(b) Cross mooring System

Fig. 10. Transmission coefficient versus (D/Hi) for all the tested models. (a) Parallel mooring System. (b) Cross mooring System

The cross-mooring setup (Fig. 10b) displays a trend that mirrors that of the parallel setup; Kt values exhibit a direct relationship with D/Hi across the full range of conditions tested. The close resemblance of the two figures indicates that the mooring layout has little effect on wave transmission when it is defined as a function of D/Hi. This means that D/Hi is the major parameter governing wave-to-structure interaction through its ability to block (as an amount of wave energy) the incoming wave energy, and this is predominantly a function of the submerged draft, with very little effect from the mooring configuration. These observed differences in Kt between the two mooring configurations under this parameter are reported on a purely empirical basis.

The three models, comparing the same D/Hi ratio, have Kt for R3 (B = 0.9 m) that achieved consistently lowest values, followed by R2 and R1. This suggests that structural width independently contributes to wave attenuation beyond the contribution of D/Hi alone, as demonstrated by this data. The scatter present for low D/Hi portrays the sensitivity of wave transmission to the individual wave parameters in the wave-to-structure interaction, particularly when the height of the incident wave is significantly greater than the submerged draft's height

3.5. Statistical Analysis

To objectively quantify the comparative predictive strength of D/B, D/L, and D/Hi, both the Pearson correlation coefficient (r) and the coefficient of determination (R^2) were calculated for each parameter against Kt across all tested models and mooring configurations. The results, summarized in Table 2, confirm that D/L consistently yields the strongest correlation under parallel mooring, with r values ranging from -0.695 to -0.765 and an average R^2 of 0.527. Under cross mooring, D/Hi showed comparable predictive strength for R1 and R2 (r = +0.545 and +0.562, respectively). When averaged across all six model-mooring combinations, D/L remained the strongest predictor overall, with an average |r| of 0.646 and an average R^2 of 0.430, compared to |r| = 0.331 and R^2 = 0.117 for D/B, and |r| = 0.475 and R^2 = 0.238 for D/Hi. These results statistically confirm that D/L is the most robust non-dimensional predictor of Kt for rectangular floating breakwaters across both mooring configurations. All correlations were statistically significant ($p < 0.05$), confirming that the observed relationships between Kt and the three governing parameters are not attributable to chance.

Table 2. Coefficient of Determination (R^2) for D/B, D/L, and D/Hi against Kt for all tested models

Model / Configuration	R^2 (D/B)	R^2 (D/L)	R^2 (D/Hi)	r (D/B)	r (D/L)	r (D/Hi)
R1 — Parallel	0.133	0.512	0.218	-0.365	-0.715	+0.467
R1 — Cross	0.049	0.272	0.297	-0.221	-0.522	+0.545
R2 — Parallel	0.128	0.586	0.248	-0.358	-0.765	+0.498
R2 — Cross	0.058	0.217	0.315	-0.240	-0.466	+0.562
R3 — Parallel	0.102	0.483	0.292	-0.319	-0.695	+0.541
R3 — Cross	0.232	0.512	0.056	-0.482	-0.715	+0.237
Average	0.117	0.430	0.238	-0.331	-0.646	+0.475

To further quantify the influence of mooring configuration on wave transmission, the percentage difference in Kt between the parallel and cross mooring arrangements was calculated for each corresponding test condition. The results show an overall average difference of 7.15% across all models and wave conditions, with individual differences reaching a maximum of 29.03% under specific wave conditions (Table 3). This confirms that mooring configuration has a measurable but relatively minor influence on Kt on average, while its effect can be more pronounced under certain wave conditions, particularly at intermediate D/L values.

Table 3. Average and maximum percentage difference in Kt between parallel and cross mooring configurations

Model	Average Difference (%)	Maximum Difference (%)
R1	6.38%	19.49%
R2	5.20%	27.42%
R3	9.87%	29.03%
Overall	7.15%	29.03%

3.6. Uncertainty Analysis

Assessing the reliability and repeatability of the experimental measurements involves selecting random test cases to repeat. One out of every ten tests was randomly selected for repetition under identical wave and model conditions, resulting in 30 repeated runs out of the 300 total tests. Following the Type A uncertainty evaluation of the GUM approach, the standard deviation between the original and repeated Kt measurements was calculated as 0.0495 (approximately 4.95%). This value is consistent with the uncertainty levels reported for ultrasonic wave gauges in laboratory flume studies (ISO & OIML, 1993; Sener et al., 2023).

3.7. Limitations

The following limitations should be considered when interpreting the results of this study:

- The models were fabricated from hollow glass sheets and do not fully replicate the material properties or mass distribution of full-scale prototype floating breakwaters.
- Experiments were conducted in fresh water under regular wave conditions, which do not represent the irregular wave spectra and salt-water environment of real coastal sites.
- Each run was limited to 60 seconds to avoid wave reflections, which does not represent sustained loading conditions in service.
- Tidal currents, wind forcing, marine corrosion, and biofouling were not considered, all of which may affect real-world performance.
- Motion-response measurements (heave, surge, pitch) were not recorded; differences in Kt between mooring configurations are therefore reported on an empirical basis only.
- The reflection coefficient (Kr) and energy dissipation coefficient (Kd) were not measured; future studies should include these to enable complete energy balance analysis.

4. Conclusions

The following conclusions are drawn from this experimental study regarding the way relative draft and mooring configuration affect the wave transmission coefficient (Kt) of rectangular pontoon floating breakwaters:

1. A consistent inverse relationship between draft and Kt was observed across all tested configurations, with reductions of up to 80% recorded at D = 20 cm compared to D = 4 cm. This confirms that draft selection is the most direct and effective geometric parameter for controlling wave attenuation in rectangular floating breakwaters, and that targeting deeper submergence depths is recommended in practical design applications.
2. Out of the two relative draft parameters that were analyzed, D/L (draft to wavelength) showed a clearer inverse trend with significantly less scatter, making it a better and more reliable predictor of Kt than D/B (draft to model width). This demonstrates that D/L is a better suitable non-dimensional design parameter for evaluating rectangular floating breakwaters' wave attenuation performance under various structural widths and wave conditions.
3. Model R3 (B = 0.9 m) consistently outperformed R1 and R2 under equivalent draft and wave conditions. Statistical analysis confirmed that structural width acts as an independent design parameter alongside draft (avg R^2 for D/B = 0.117 vs avg R^2 for D/L = 0.430), and that maximizing both width and draft simultaneously produces the most effective wave protection. These findings suggest that wider rectangular floating breakwaters with deeper drafts should be prioritized to achieve optimal wave attenuation performance.
4. A positive relationship with Kt was exhibited in the D/Hi (draft-to-incident wave height ratio), with lower D/Hi values resulting in higher levels of wave-structure interaction and more effective wave attenuation due to an increased ratio of the incident wave height relative to the draft.
5. In terms of wave attenuation, the cross-mooring configuration produced empirically lower Kt values than the parallel arrangement across most tested conditions, particularly when results were expressed as a function of draft and D/B. The overall average percentage difference between the two configurations was 7.15%, with a maximum of 29.03% under specific wave conditions. This difference diminished when Kt was expressed in terms of D/L. As motion-response measurements were not conducted in the present study, the observed differences are reported on a purely empirical basis.

Reference

Abasi, N., Ershadi, C., Lotfollahi Yaghin, M.A., & Mojtahedi, A. (2023). Experimental and Numerical Investigation of Degree of Freedom Effects on Hydrodynamic Performance of Floating Breakwaters Under Regular Waves. *International Journal Of Coastal, Offshore And Environmental Engineering (Ijcoe)*, *8*(1), 45–60.

Chen, Q., Zang, J., Birchall, J., Ning, D., Zhao, X., & Gao, J. (2020). On the hydrodynamic performance of a vertical pile-restrained WEC-type floating breakwater. *Renewable Energy*, *146*, 414–425.

Cheng, X., Li, S., Xie, W., Xu, C., Wang, J., & Xu, T. (2025). Numerical Simulation Study of the Hydrodynamic Properties of a Floating Breakwater of Pontoons. *Polish Maritime Research*.

Cheng, Y., Fu, L., Dai, S., Collu, M., Ji, C., Yuan, Z., & Incecik, A. (2022). Experimental and numerical investigation of WEC-type floating breakwaters: A single-pontoon oscillating buoy and a dual-pontoon oscillating water column. *Coastal Engineering*, *177*, 104188. https://doi.org/https://doi.org/10.1016/j.coastaleng.2022.104188

Dai, J., Wang, C. M., Utsunomiya, T., & Duan, W. (2018). *Review of recent research and developments on floating breakwaters*. In Ocean Engineering (Vol. 158, pp. 132–151). Elsevier Ltd. https://doi.org/10.1016/j.oceaneng.2018.03.083

Duan, W., Xu, S., Xu, Q., Ertekin, R.C., & Ma, S. (2017). Performance of an F-type floating breakwater: A numerical and experimental study. Proceedings of the Institution of Mechanical Engineers, Part M: *Journal of Engineering for the Maritime Environment*, *231*(2), 583–599.

Ji, C., Deng, X., & Cheng, Y. (2019). An experimental study of double-row floating breakwaters. *Journal of Marine Science and Technology* (Japan), *24*(2), 359–371. https://doi.org/10.1007/s00773-018-0554-2

Lee, C.F., & Ong, M.C. (2025). Numerical analysis of mooring systems for reducing peak mooring line tensions in a combined wind and wave energy system at an intermediate water depth. *Ocean Engineering*, *325*, 120767.

Nasri, B., Moghim, M.N., & Badri, M.A. (2021). Experimental study on trapezoidal pontoon-type floating breakwaters with attached porous plates. *Journal of Ocean Engineering and Marine Energy*, *7*(1), 41–57. https://doi.org/10.1007/s40722-021-00185-z

Nikpour, A.H., Moghim, M.N., & Badri, M.A. (2019). Experimental Study of Wave Attenuation in Trapezoidal Floating Breakwaters. *China Ocean Engineering*, *33*(1), 103–113. https://doi.org/10.1007/s13344-019-0011-y

Rajabi, M., & Ghassemi, H. (2021). Hydrodynamic Performance Improvement of Double-Row Floating Breakwaters by Changing the Cross-Sectional Geometry. *Mathematical Problems in Engineering*, 2021. https://doi.org/10.1155/2021/2944466

Ren, J., Jin, P., Liu, Y., & Zang, J. (2021). Wave attenuation and focusing by a parabolic arc pontoon breakwater. *Energy*, *217*, 119405. https://doi.org/https://doi.org/10.1016/j.energy.2020.119405

Saie, Y. El, Sayed, A. El, Ehab, H., & Balah, A. (2023). The Hydrodynamic Performance Examination of a New Floating Breakwater Configuration. *International Journal of Advanced Engineering, Management and Science*, *9*(1), 01–08. https://doi.org/10.22161/ijaems.91.1

Sannasiraj, S.A., Sundar, V., & Sundaravadivelu, R. (1998). Mooring forces and motion responses of pontoon-type floating breakwaters. *Ocean Engineering*, *25*(1), 27–48.

Shen, Y., Pan, J., Zhou, Y., & Wang, X. (2022). Experimental Study on Wave Attenuation Performance of A New Type of Floating Breakwater with Twin Pontoons and Multi Porous Vertical Plates. *China Ocean Engineering*, *36*(3), 384–394. https://doi.org/10.1007/s13344-022-0034-7

Wang, Y., Ji, C., Xu, S., & Mao, R. (2025). Theoretical Study on the Wave Attenuation Performance of Floating Breakwater with a Rectangular Cross-Section. *China Ocean Engineering*, *39*(2), 244–255. https://doi.org/10.1007/s13344-025-0034-5

Xu, W., Sun, Y., He, Z., Zhang, X., Gao, X., & Liu, R. (2024). Dynamic Response Analysis of A Floating Photovoltaic System with Different Mooring Arrangements in An Area with Large Tidal Variations. *China Ocean Engineering*, *38*(6), 1057–1070. https://doi.org/10.1007/s13344-024-0083-1